Research Square

Preprints are preliminary reports that have not undergone peer review.
They should not be considered conclusive, used to inform clinical practice,
or referenced by the media as validated information.

Comparative Analysis of Bidirectional and Hybrid Pumping Schemes for Pre-Amplifier EDFAs: ASE-Induced Gain Saturation Dynamics

Jaba Das
University of Dhaka
Asiful Islam
University of Dhaka
Sazzad M.S. Imran
sazzadmsi@du.ac.bd
University of Dhaka

Research Article

Keywords: Erbium-Doped Fiber Amplifiers (EDFAs), Population Inversion, Bidirectional Pumping, Hybrid Pumping, Signal Gain, Amplified Spontaneous Emission (ASE).

Posted Date: August 6th, 2026

DOI: https://doi.org/10.21203/rs.3.rs-10502117/v1

License: This work is licensed under a Creative Commons Attribution 4.0 International License.
Read Full License

Additional Declarations: No competing interests reported.

Version of Record: A version of this preprint was published at Optical and Quantum Electronics on October 12th, 2026. See the published version at https://doi.org/10.1007/s11082-026-09192-6.

Comparative Analysis of Bidirectional and Hybrid Pumping Schemes for Pre-Amplifier EDFAs: ASE-Induced Gain Saturation Dynamics

Jaba Das[1], Asiful Islam[2], Sazzad M.S. Imran[3*]

[1, 2, 3]Dept. of Electrical and Electronic Engineering, University of Dhaka, Bangladesh

[*]Corresponding author: sazzadmsi@du.ac.bd

Abstract:

In this paper we present detailed numerical study of the spatial gain dynamics, ASE (amplified spontaneous emission) evolution and NF (noise figure) characteristics of erbium-doped-fiber-amplifiers (EDFAs) operating in the pre-amplifier regime with input signal power -40 dBm. We first perform parametric analysis of signal gain under bidirectional (1480 nm and 980 nm) and hybrid (1480 nm forward + 980 nm backward and 980 nm forward + 1480 nm backward) pumping configurations for four different EDFA lengths of 5, 10, 15 and 20 m. We solve two-level rate equation EDFA model using the fourth-order Runge-Kutta method (RK4) with iterative forward-backward ASE and pump integration. The results validate that 20 m long EDFA with 1480 nm forward pumping provides optimum gain. Our results reveal 15 m as threshold length beyond which hybrid scheme outperforms bidirectional configuration for 35% to 80% 1480 nm forward pump fraction. This is attributed to the higher ASE build up beyond 15 m causes gain saturation for bidirectional pumping. However for 80% and above pump fraction, both hybrid and bidirectional schemes show nearly identical gain performance. This is because of rapid absorption of the 980 nm backward pump in the first 5 m creates asymmetric pump distribution that suppresses ASE buildup in the latter half of the fiber. The 980 nm forward pumping is suitable for 10 m long EDFA though it performs poorly for 20 m length due to rapid pump depletion and signal reabsorption. These results provide practical guidelines for EDFA operation in optical communication system.

Keywords:

Erbium-Doped Fiber Amplifiers (EDFAs), Population Inversion, Bidirectional Pumping, Hybrid Pumping, Signal Gain, Amplified Spontaneous Emission (ASE).

Introduction:

Erbium-Doped Fiber Amplifiers (EDFAs) play a crucial role in modern long-haul optical communication systems, contributing significantly to the lossless data transmission [1-2]. Operating within the erbium absorption bands of 980 nm and 1480 nm, EDFAs offer high gain, low noise and wide bandwidth in wavelength-division multiplexing (WDM) networks [2-4]. Among the various applications of EDFA, pre-amplifiers are of crucial importance in improving receiver sensitivity by amplifying weak signals before detection, that requires

very low noise figures (typically < 4 dB) and high small-signal gain [2, 5]. Despite years of development, EDFAs remain a focus of ongoing research to improve their efficiency and lower noise for fiber lengths of 10 to 30 m, as well as for dual-wavelength bidirectional pumping [5-18].

Masuda et al. demonstrated a large unsaturated net gain of 51 dB for a 1550 nm signal using a two-stage EDFA configuration pumped by 1480 nm laser diodes [5]. Based on this success, Delavaux et al. presented a comprehensive study of multi-stage EDFAs showing gains, power conversion efficiency and noise figure improvements [6]. Myslinski et al. [7] have studied extensively the dependence of EDFA performance on the erbium ion concentration, signal wavelength and the relative direction of the pump and signal beams. Gain dynamics have been studied extensively with respect to erbium concentration, pump configurations and fiber length [3, 8-16]. Bidirectional pumping generally yields better gain and noise performance [12, 17]. Pradhan et al. [8] and Lavrinovica et al. [9] highlight influence of different pumping schemes on gain saturation and noise figure. Improved gain saturation and efficiency of cladding-pumped EDFA systems have been shown by Zakis et al. [10]. Jalilpiran et al. [11] also optimized the L-band EDFAs by analyzing the excited-state absorption and the improvement of erbium solubility. A detailed analysis of the input signal power in a cascaded EDFA simulation model with various pumping techniques was carried out by Semmalar et al. [13]. Awsaj et al. studied the gain and noise figure characteristics of an EDFA in the L-band by examining the effect of a double pass configuration [14]. Liu et al. classified the EDFA models into analytical modeling and machine learning (ML) based modeling [15].

Further progress in the EDFA technology has been made in recent research through development of advanced fiber designs, gain optimization methods and sophisticated numerical modeling approaches. The different amplification properties of 980 nm and 1480 nm pumping schemes were discussed by Zhai et al. [19]. Trinel et al. have demonstrated that optimized fiber geometries can increase the amplification in EDFAs [20]. Lao et al. reported improved gain characteristics in extended L-band EDFAs in which dual stage double pass configuration has been used [21]. Gu et al. [22] presented novel EDFA architectures for high-efficiency amplification, while Li et al. proposed tunable gain-clamped EDFA architectures with improved gain stability [23].

Although a lot of progress has been achieved in the optimization and design of EDFAs, a detailed spatial analysis of population inversion and gain dynamics in pre-amplifier EDFAs is still absent for intermediate fiber lengths (e.g. 20 m) under hybrid pumping with simultaneous 980 nm and 1480 nm excitation. Specifically, the interaction among spatial inversion distribution, ASE induced gain saturation and length dependent performance in pre-amplifier EDFAs for dual-wavelength (980/1480 nm) bidirectional pumping strategy is not fully characterized.

The goal of this study is to fill that gap by a systematic analysis of pre-amplifier EDFA under bidirectional and hybrid pumping at 1480 nm and 980 nm excitation. We assume -40 dBm input signal power and 20 mW total pump power that are typical for pre-amplifier applications. We emphasize that our results are length specific and do not contradict with

the well-established use of 980 nm forward pumping in shorter-EDFA pre-amplifiers [17, 18]. The results indicate a distinct transition in the amplifier behavior at about 15 m EDFA length. We also study the noise figure and signal gain as a function of the forward pump power fraction from 0% to 100%. We choose 5, 10, 15 and 20 m to study the length dependent performance.

We organized the paper as follows: Section I points out the breakthroughs and advances in EDFA researches. The mathematical model and rate equations describing the population inversion and field propagation in EDFAs are presented in Section II. Section III describes the numerical methods used, i.e., the fourth order Runge-Kutta method. Section IV presents a detailed analysis and interpretation of the simulation results. Section V summarizes the results of the study as well as the achievements of the work.

Theory and Mathematical Model:

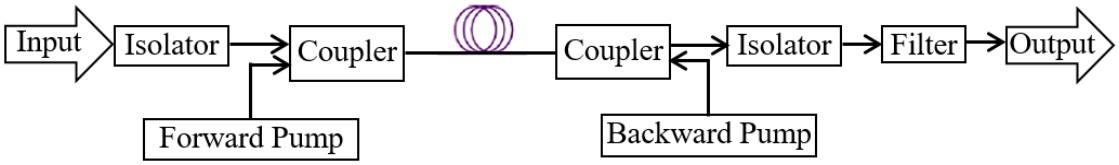


Fig. 1: A schematic diagram of a basic EDFA configuration with simultaneous forward and backward pumping. This configuration enables single wavelength bidirectional pumping and dual wavelength hybrid pumping.

The operational principle of an EDFA is illustrated in Fig. 1, in which main component is the EDF, where Er^{3+} are embedded into the core [1, 2, 4, 21]. When stimulated by pump source, the energy elevates erbium ions to higher energy levels, with common pump wavelengths for EDFAs typically residing around 980 nm and 1480 nm [5, 22]. The information-carrying optical signals is typically within the erbium absorption band, commonly around 1550 nm [6, 23]. The overall amplification process is characterized by the absorption and emission cross-sections, lifetimes of energy states and the spatial distribution of erbium ions within the fiber [3, 24].

EDFA operation is described by a three-level systems – ground state, pump band and metastable state. We can approximate the three-level system to an effective two-level system assuming fast non-radiative relaxation from the pump band to metastable state [17, 18]. Population inversion equation of EDFAs, considering two-level system, is given by:

$$N_2(z) = \frac{\frac{\tau\sigma_s^a}{Ah\nu_s}\Gamma_s P_s + \frac{\tau\sigma_j^a}{Ah\nu_j}\Gamma_{\nu j} P_A(\nu_j) + \frac{\tau\sigma_p^a}{Ah\nu_p}\Gamma_p P_p}{\frac{\tau(\sigma_s^a+\sigma_s^e)}{Ah\nu_s}\Gamma_s P_s + \frac{\tau\left(\sigma_{\nu_j}^a+\sigma_{\nu_j}^e\right)}{Ah\nu_j}\Gamma_{\nu_j} P_A(\nu_j) + \frac{\tau\left(\sigma_p^a+\sigma_p^e\right)}{Ah\nu_p}\Gamma_p P_p + 1} N \qquad (1)$$

where Γ_s is the overlap factor between erbium distribution and signal field mode, Γ_p is the overlap factor between erbium distribution and pump field mode, $A = \pi R^2$ is the effective area of the erbium distribution with R = radius of Er^{3+} distribution ≤ core-radius. σ_p^a and σ_s^a are the absorption cross-sections for pump and signal, σ_p^e and σ_s^e are emission cross-

sections for pump and signal, τ is the lifetime of the upper-level, h is the Planck's constant, ν is the frequency, P is the power and N is the total Er^{3+} ion concentration.

Field propagation equations in terms of field powers are given by:

$$\frac{dP_p}{dz} = \left(N_2\sigma_p^{(e)} - N_1\sigma_p^{(a)}\right)\Gamma_p P_p - \alpha_p^{(a0)}P_p \quad (2)$$

$$\frac{dP_s}{dz} = \left(N_2\sigma_s^{(e)} - N_1\sigma_s^{(a)}\right)\Gamma_s P_s - \alpha_s^{(a0)}P_s \quad (3)$$

$$\frac{dP_A^+(v_j)}{dz} = \left(N_2\sigma_{v_j}^{(e)} - N_1\sigma_{v_j}^{(a)}\right)\Gamma_s P_A^+(v_j) + N_2\sigma_{v_j}^{(e)}\Gamma_s h v_j\,\Delta v_j - \alpha_{v_j}^{(a0)}P_A^+(v_j) \quad (4)$$

$$\frac{dP_A^-(v_j)}{dz} = -\left(N_2\sigma_{vj}^{(e)} - N_1\sigma_{vj}^{(a)}\right)\Gamma_s P_A^-(v_j) - N_2\sigma_{vj}^{(e)}\Gamma_s h v_j\,\Delta v_j + \alpha_{v_j}^{(a0)}P_A^-(v_j) \quad (5)$$

Assuming zero background loss, the total signal gain can be expressed as

$$G = 10log_{10}\left(\frac{P_s(L)}{P_s(0)}\right)\,[dB] \quad (6)$$

where N_2 is the upper-state population, $N_1 = N - N_2$ is the lower-state population, $P_A^+(v_j)$ is the forward traveling ASE and $P_A^-(v_j)$ is the backward travelling ASE at frequency ν_j, and $\alpha_p^{(a0)}$, $\alpha_s^{(a0)}$ and $\alpha_{v_j}^{(a0)}$ are the possible intrinsic background loss in the fiber at pump, signal and ASE wavelength, respectively.

The noise figure (NF) is calculated as

$$NF_{dB} = 10log_{10}\left[2n_{sp}\frac{G-1}{G} + \frac{1}{G}\right] \quad (7)$$

where $G = \frac{P_{s,out}}{P_{s,in}}$ is the signal gain and $n_{sp} = \frac{N_2}{N_2 - N_1}$ is the spontaneous emission factor.

Assuming no emission at 980 nm, we set $\sigma_{p,980}^e = 0$ for hybrid (1480 nm forward + 980 nm backward) pumping configuration. Population inversion for hybrid pumping, therefore, can be expressed as

$$N_2 = \frac{\frac{\tau\sigma_s^a\Gamma_s}{Ah\nu_s}P_s + \frac{\tau\sigma_{p,980}^a\Gamma_{p,980}}{Ah\nu_{980}}P_{980} + \frac{\tau\sigma_{p,1480}^a\Gamma_{p,1480}}{Ah\nu_{1480}}P_{1480}}{\frac{\tau(\sigma_s^a+\sigma_s^e)\Gamma_s}{Ah\nu_s}P_s + \frac{\tau\sigma_{p,980}^a\Gamma_{p,980}}{Ah\nu_{980}}P_{980} + \frac{\tau\left(\sigma_{p,1480}^a+\sigma_{p,1480}^e\right)\Gamma_{p,1480}}{Ah\nu_{1480}}P_{1480}+1}N \quad (8)$$

In our simulation, we assume uniform Er^{3+} distribution within the core radius and neglect the background losses in gain calculation.

Numerical Simulation Method:

The analytical solution for nonlinear coupled differential equations (2) to (5) is not feasible. Because these equations depend on signal and pump power which themselves evolve along the EDFA length. Therefore, we solve the system equations through the fourth order Runge-Kutta method (RK4 method) which can be defined as

$$y_{n+1} = y_n + \frac{1}{6}(k_1 + 2k_2 + 2k_3 + k_4) \quad (9)$$

where $k_1 = hf(x_n, y_n)$, $k_2 = hf\left(x_n + \frac{1}{2}h, y_n + \frac{1}{2}k_1\right)$, $k_3 = hf\left(x_n + \frac{1}{2}h, y_n + \frac{1}{2}k_2\right)$, $k_4 = hf(x_n + h, y_n + k_3)$, h is the simulation step-size, and $f()$ is the right-side of the differential equations.

Because ASE propagates in both forward and backward directions and we don't know exact value of backward ASE at z = 0 a priori, we first calculate the forward-propagating ASE at z = 0 assuming $P_A^- = 0$. Then we calculate the backward-propagating ASE using the forward ASE results. Now we repeat the forward and backward simulations many times until the relative change in the amplified power $P_A^+(v_j)$ at frequency v_j between successive iterations is less than 10^{-6}.

$$\frac{|P_A^{x+1}(v_j) - P_A^x(v_j)|}{P_A^x(v_j)} < 10^{-6} \qquad \text{for } P_A^x(v_j) > 0 \tag{10}$$

where x is the iteration number. As we assume the ASE power is zero at the start of iteration, the criterion is applied once the power becomes non-zero. Typically, convergence is achieved in 12-18 iterations with maximum number of iterations is 30.

Table 1: Physical and optical parameters used in the simulation [17, 18]

Pump absorption σ_p^a at 980 nm	2.7×10^{-21} cm²
Pump emission σ_p^e at 980 nm	0
Pump absorption σ_p^a at 1480 nm	1.5×10^{-21} cm²
Pump emission σ_p^e at 1480 nm	0.5×10^{-21} cm²
Signal absorption σ_s^a at 1550 nm	2.8×10^{-21} cm²
Signal emission σ_s^e at 1550 nm	1.9×10^{-21} cm²
Core-radius	1.4 μm
Signal overlap factor Γ_s at 1550 nm	0.64
Pump overlap factor Γ_p at 1480 nm	0.77
Pump overlap factor Γ_p at 980 nm	0.86
Er^{3+} concentration N	4×10^{19} cm^{-3}
Input signal power $P_s(0)$	-40 dBm (pre-amplifier regime)
Total pump power (P_{total})	20 mW
Fiber length studied	5, 10, 15 and 20 m

Results and Discussion:

Fig. 2 shows evaluation of signal gain with different pump power fraction from 0% to 100% for four different EDFA lengths (5, 10, 15 and 20 m). Simulation was done for different bidirectional (980 nm forward + backward, and 1480 nm forward + backward) and hybrid

(980 nm forward + 1480 nm backward and 1480 nm forward + 980 nm backward) pumping configurations. This parametric analysis was done to justify our length choice for next simulation. Results confirm that for 980 nm forward pumping, EDFA length of 10 m shows favorable gain for different pump fraction, and for 1480 nm forward pumping, EDFA length of 20 m shows optimum signal gain for 60% or more forward pump fraction. This demonstrate the advantage of using 1480 nm as forward pump power for both bidirectional (1480 nm backward pumping) and hybrid (980 nm backward pumping) configurations for 20 m long EDFA. On the other hand, for 10 m shorter length EDFA, using 980 nm as forward pumping is advantageous for both bidirectional and hybrid pumping schemes.

Hybrid (1480 nm forward + 980 nm backward) pumping shows the best performance among all four configurations. The forward pump at 1480 nm has a deep penetration into the fiber while the backward pump at 980 nm is absorbed rapidly near the output end, leading to a complementary pumping profile. For 20 m fibers, 980 nm bidirectional pumping is inefficient due to fast pump depletion near the input. Nevertheless, it exhibits a reasonable performance at 5-10 m, confirming the suitability of 980 nm pumping for shorter fibers.

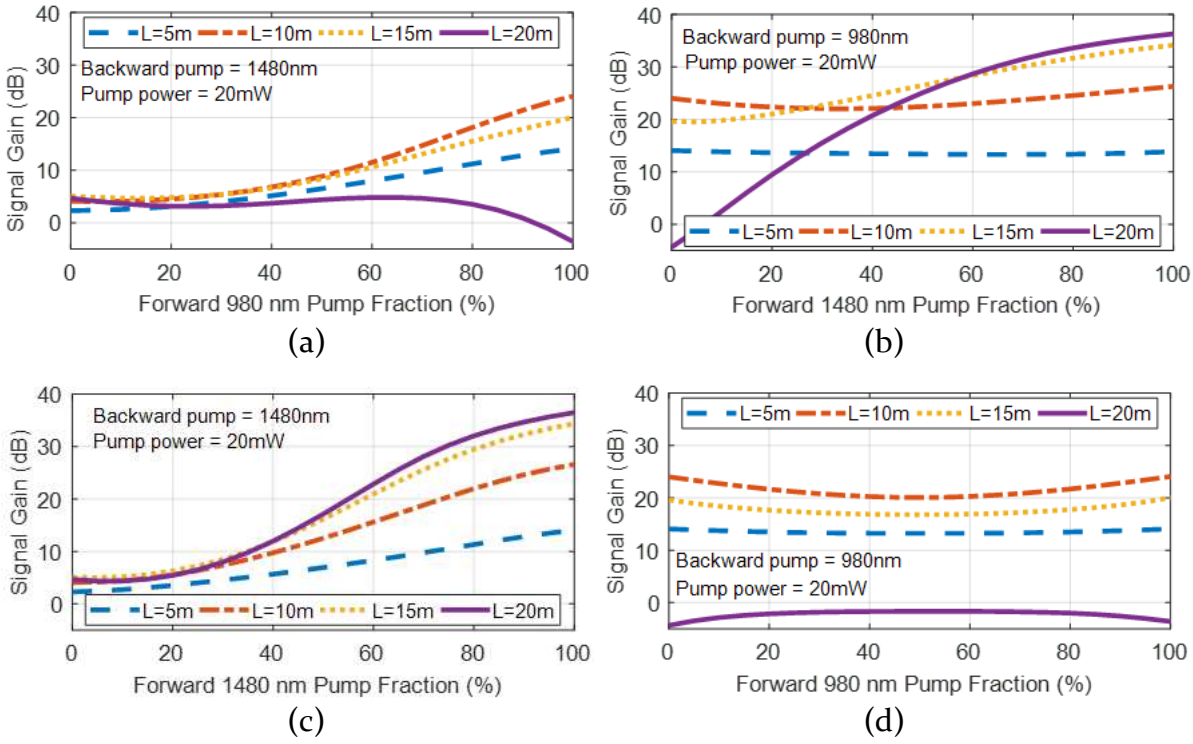


Fig. 2: Output signal gain as a function of pump power ratio for four different EDFA length with forward pump fraction varies from 0% to 100%, and -40 dBm input signal power. (a) Hybrid (980 nm forward + 1480 nm backward) pumping. (b) Hybrid (1480 nm forward + 980 nm backward) pumping. (c) 1480 nm bidirectional pumping. (d) 980 nm bidirectional pumping.

Based on signal gain evaluation for different EDFA lengths shown in Fig. 2, we select 20 m length for 1480 nm forward pumping configurations and 10 m length for 980 nm forward

pumping configurations for further investigation. Fig. 3 shows evaluation of the signal gain and noise figure with different pump power fraction from 0% to 100% for these selected configurations. The results reveal that the choice of forward pump wavelength has a dominant influence on EDFA gain performance as it determines the population inversion distribution across the fiber. Results in Fig. 2 and Fig. 3 demonstrate that using 980 nm as forward pumping is suitable for 10 m long EDFA applications. This is attributed to the rapid absorption of 980 nm pump near the fiber input beyond 10 m length. As a result the inversion becomes highly localized and the effective gain length is reduced because the signal is reabsorbed in the remaining fiber length. Thus the signal gain remains below 5 dB for a 20 m long EDFA. For hybrid (980 nm forward + 1480 nm backward) pumping (Fig. 3(a)) the signal gain is less than 5 dB and for 980 nm bidirectional pumping (Fig. 3(d)) there is no signal gain for 20 m EDFA and 20 mW total pump power. The noise figure is above 4 dB for both cases.

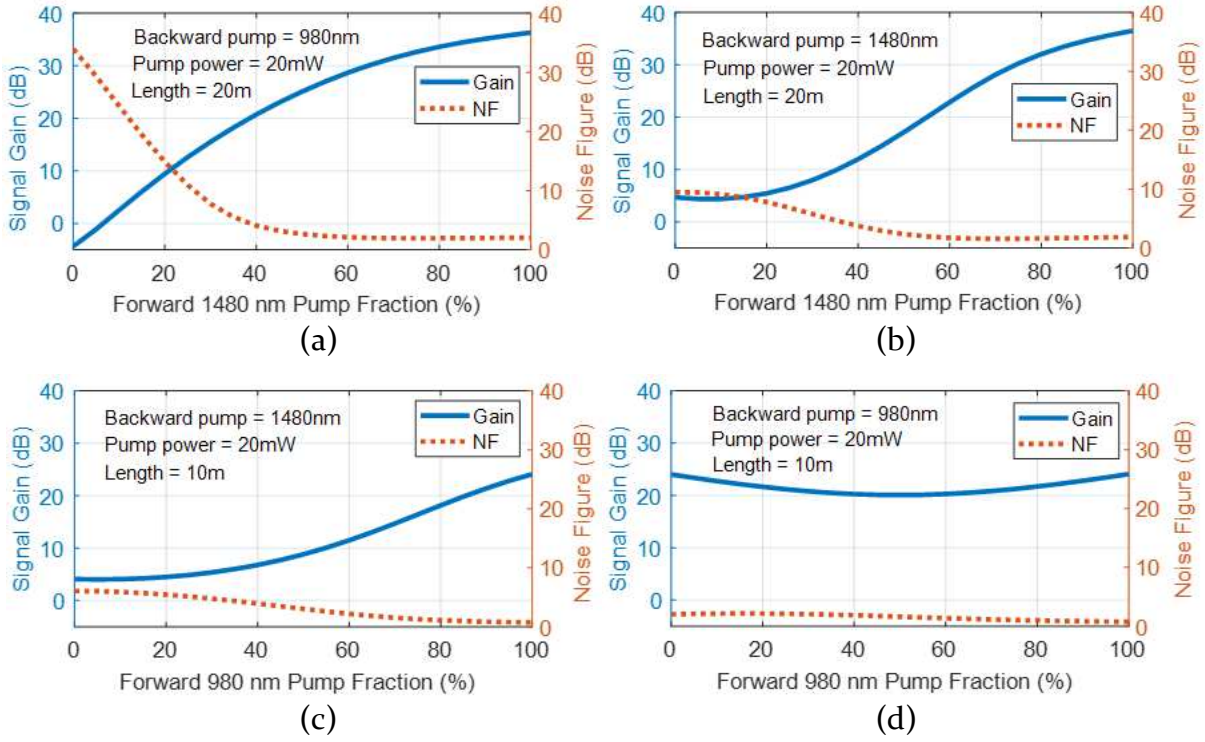


Fig. 3: Output signal gain and noise figure as a function of pump power ratio with forward pump fraction varies from 0% to 100% with -40 dBm input signal. (a) Hybrid (1480 nm forward + 980 nm backward) pumping for 20 m EDFA. (b) 1480 nm bidirectional pumping with 20 m EDFA. (c) Hybrid (980 nm forward + 1480 nm backward) pumping for 10 m EDFA. (d) 980 nm bidirectional pumping for 10 m EDFA.

On the other hand, using 1480 nm as forward pumping yields signal gain above 10 dB and noise figure below 3 dB for 35% and above forward 1480 nm pump fraction and therefore, suitable for 20 m long EDFA applications. Lower absorption of 1480 nm pump allows it to penetrate deeper into the fiber resulting more uniform inversion distribution along the fiber. This enables efficient signal amplification over a larger fraction of the fiber length.

The observed reduction of NF with the increase of forward pump fraction is again attributed to more localized pump absorption that increases inversion near the signal input. This reduces reabsorption of signal photon and hence the spontaneous emission, thus reducing the NF below 3 dB.

For 20 m long EDFA, both hybrid and bidirectional pumping show below par performance below 35% 1480 nm forward pump fraction in terms of signal power and NF as in that regime either signal power is below 10 dB or NF is above 5 dB. Hybrid pumping shows superior performance compare to bidirectional pumping from 35% to 80% 1480 nm forward pump fraction. In that region signal gain is above 10 dB and NF is below 5 dB. However, as we increase the 1480 nm forward pump fraction further from 80%, both hybrid and bidirectional pumping perform equally.

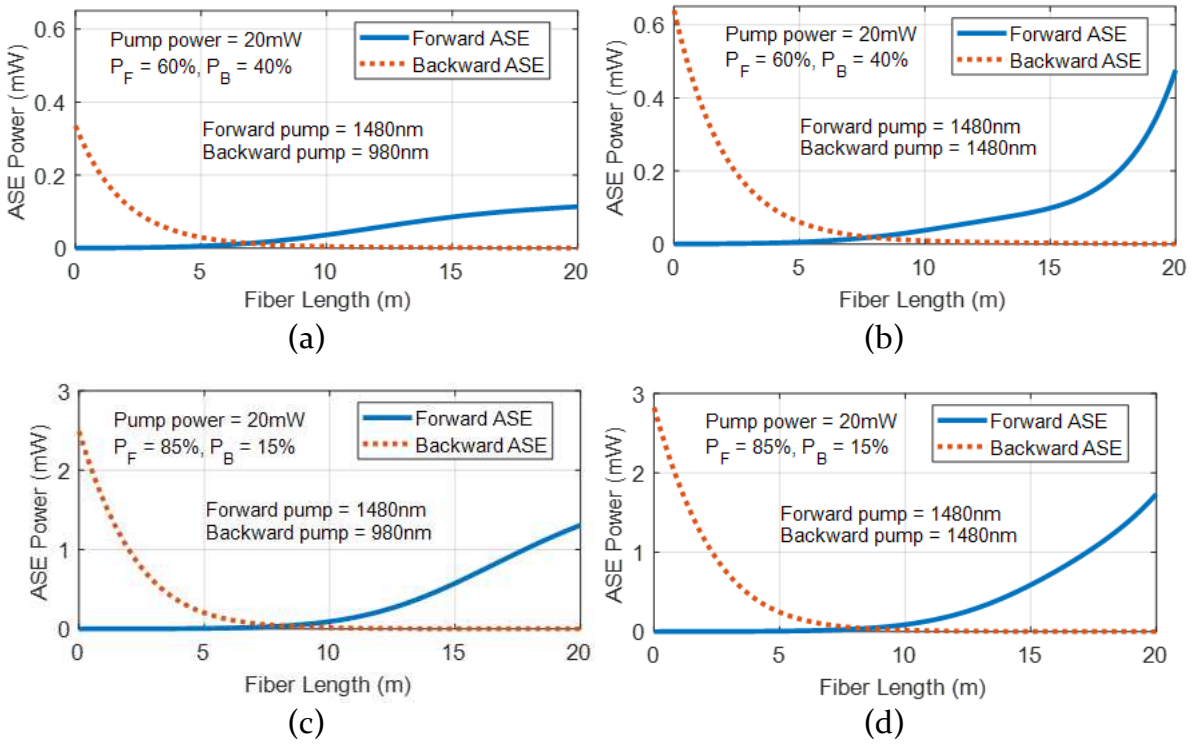


Fig. 4: Evolution of forward and backward ASE buildup along the EDFA length for 20 mW total pump power. (a) Hybrid (1480 nm forward + 980 nm backward) pumping with 60% forward pump fraction. (b) 1480 nm bidirectional pumping with 60% forward pump fraction. (c) Hybrid (1480 nm forward + 980 nm backward) pumping with 85% forward pump fraction. (d) 1480 nm bidirectional pumping with 85% forward pump fraction.

Fig. 4 show evolution of forward and backward ASE buildup across EDFA for bidirectional and hybrid pumping for two different forward pump power fractions. It is to mention that the ASE originates from the spontaneous emission and directly compete with the signal for the available population inversion. At 60% forward fraction, the hybrid configuration suppresses ASE through asymmetric pump distribution because strong absorption of 980 nm backward pump near output. This reduced ASE accumulation preserves population inversion and delays gain saturation. For bidirectional pumping we got higher ASE after 15

m because of enhanced ASE after 15 m that causes robbing of higher fraction of population inversion, resulting in gain saturation. At 85% forward fraction, both configurations show nearly similar ASE distribution because the backward pump power (15% of total) is insufficient to create significant asymmetry.

Fig. 5 shows population inversion distribution across the EDFA and confirms the ASE induced gain saturation mechanism and the gain behavior observed in Fig. 6. At 60% forward pump fraction, the ASE suppression in hybrid configuration preserves inversion beyond 15 m. But the enhanced ASE in the 1480 nm bidirectional pumping consumes large fraction of Er^{3+} population causing inversion level to decrease continuously. On the other hand, both configurations behave similarly at 85% forward fraction because the backward pump is too weak to create ASE suppression.

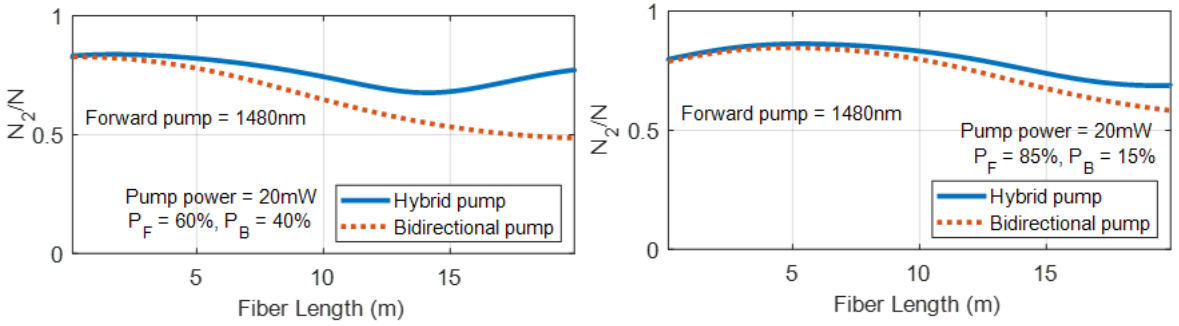


Fig. 5: Normalized population inversion distribution along EDFA length for hybrid (1480 nm forward + 980 nm backward) pumping and 1480 nm bidirectional pumping with (a) 60% forward pump fraction and (b) 85% forward pump fraction.

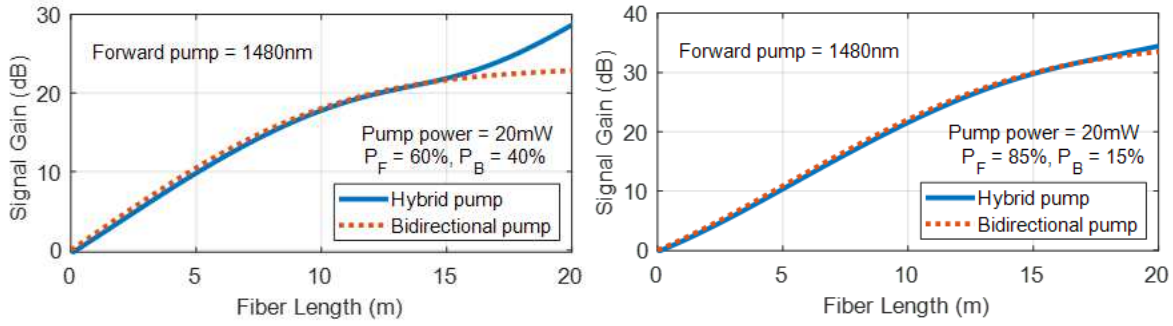


Fig. 6: 1550 nm signal gain evolution along EDFA length for 1480 nm bidirectional pumping, and hybrid (1480 nm forward + 980 nm backward) pumping with (a) 60% forward pump fraction and (b) 85% forward pump fraction.

Fig. 6 shows 1550 nm signal gain evolution along EDFA length for both hybrid and bidirectional pumping at 60% and 85% forward pump fractions. The results demonstrate the effect of inversion distribution profile in Fig. 5 on signal gain. At 60% forward pump fraction, up to 15 m EDFA length both configurations exhibit identical gain performance due to similar population inversion distribution. But after 15 m, the signal gain for EDFA

with bidirectional pumping becomes saturated because the stronger ASE depletes the available inversion. In contrast, the signal gain for EDFA with hybrid pumping continue to increase due to weaker ASE build up and therefore availability of higher inversion level. Consequently, for EDFA length exceeding 15 m, hybrid (1480 nm forward + 980 nm backward) pumping exhibits superior gain performance as compared to 1480 nm bidirectional pumping due to reduced ASE induced gain saturation. At 85% forward fraction, both configurations perform identically because the backward pump is too weak to affect ASE dynamics.

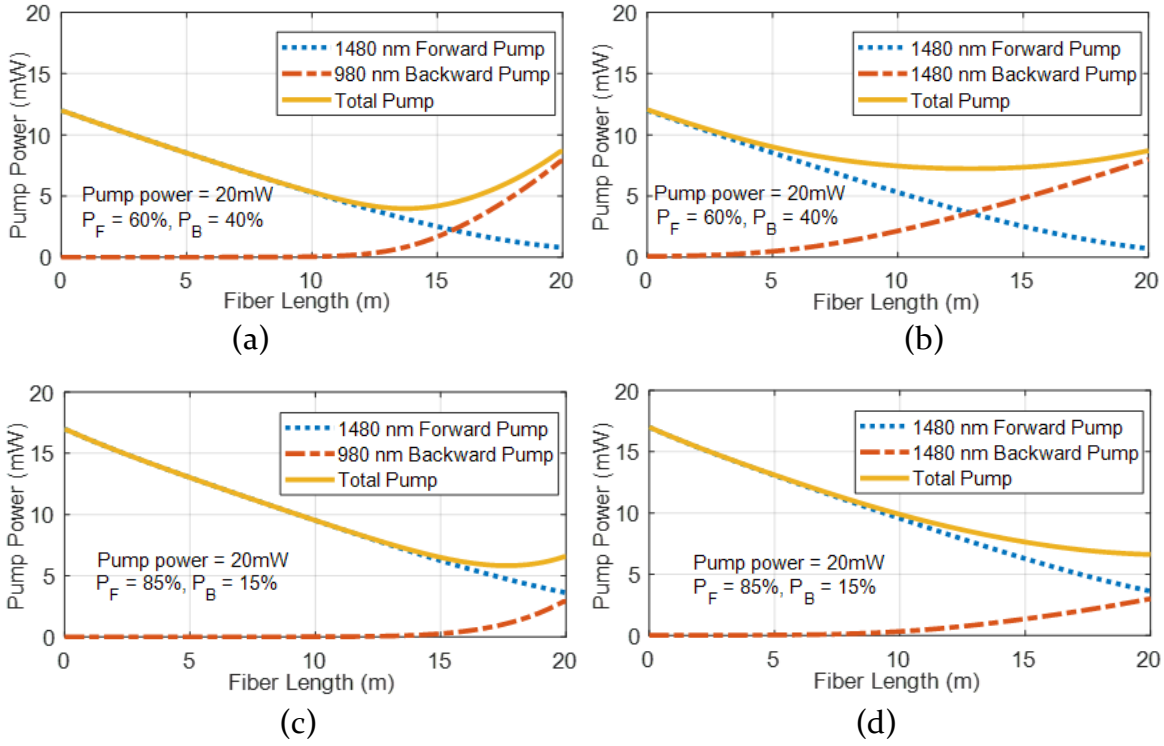


Fig. 7: Pump power evolution along EDFA length for (a) Hybrid (1480 nm forward + 980 nm backward) with 60% forward pump fraction. (b) 1480 nm bidirectional pumping with 60% forward pump fraction. (c) Hybrid (1480 nm forward + 980 nm backward) with 85% forward pump fraction. (d) 1480 nm bidirectional pumping with 85% forward pump fraction.

Fig. 7(a) and 7(b) show evolution across EDFA for forward, backward and total pump power under both bidirectional and hybrid pumping at 60% and 85% forward pump fractions with 20 mW total pump power. At 60% forward pump fraction, 980 nm backward pump in hybrid pumping absorbed rapidly within first 5 m due to higher absorption coefficient creating a pump power dip at 15 m length. However, bidirectional pumping showed relatively uniform power distribution across the EDFA. At 85% forward pump fraction, backward pump (15% of total) is too weak to create significant asymmetry, therefore got forward-dominant pumping behavior.

Becker et al. [18] reported gains up to 28 dB for a 14 m fiber with 20 mW 980 nm pump power. Our results show up to 24 dB signal gain for 10 m fiber with 980 nm forward

pumping. For 20 m fiber, 980 nm pumping yields only 5 dB gain due to signal reabsorption. This confirms that our 980 nm results are length-specific and consistent with established literature.

Conclusion:

This paper has presented comprehensive numerical analysis of spatial evolution of population inversion, pump absorption, ASE and signal gain in Al-Ge-Er-doped Si fiber based EDFA operating in the pre-amplifier regime (-40 dBm input signal) under bidirectional and hybrid pumping configurations. We solved approximate two-level rate equation EDFA model through the fourth order Runge-Kutta method where we varied forward pump power fraction from 0% to 100%.

We derive 15 m threshold fiber length above which ASE effects are expected to be significant. At 60% forward pump fraction, hybrid pumping achieved approximately 6 dB higher gain than bidirectional pumping beyond 15 m EDFA length while maintaining NF below 3 dB, because reduced ASE allows continued population inversion and gain growth. Before 15 m both pumping schemes showed identical gain performance. The 980 nm backward pump in hybrid configuration is rapidly absorbed within the first 5 m that creates a non-uniform pump distribution. However, at 85% forward fraction the two configurations behave the same as the backward pump is too weak to affect ASE dynamics. We got less than 5 dB gain for 20 m fiber with 980 nm forward pumping. However, at 10 m length it gains up to 24 dB confirming the limitation is length specific.

Thus, we establish the spatial mechanism by which ASE induced inversion depletion governs gain saturation in intermediate length pre-amplifier EDFAs. The forward fraction dependence of performance gives practical design guidance: pump wavelength asymmetry (1480/980 nm) can suppress ASE-driven saturation past 15 m critical length, but only when the backward pump power is large enough (> ~20% of total).

Author Contributions: J.D. and A.I. performed the numerical simulations. S.M.S.I. provided the idea and wrote the manuscript including interpretation of the results. All authors reviewed the manuscript and approved the final version of the manuscript.

Funding: The authors declare that no funds, grants, or other financial support were received during this research or the preparation of this manuscript.

Data Availability: The simulation (numerical) datasets generated and/or analyzed during the current study are available from the corresponding author on reasonable request.

Conflict of Interest: The authors declare that they have no competing interests.

References:

1) A.J. Bruce and R. Wyatt, Recent advances in erbium-doped fiber amplifies and their applications, Progress in Quantum Electronics, vol. 28, no. 2, pp. 63-108, 2004.

2) J. Nilsson, Erbium-doped fiber amplifiers: principles and applications, Laser & Photonics Reviews, vol. 1, no. 2, pp. 234-258, 2007.

3) L. Zhang, Y. Du, Y. Xi, C.W. Zhao and J. Li, Gain characteristic of erbium doped fiber amplifier, Proceedings of SPIE – The International Society for Optical Engineering, vol. 7157, pp. 715714-1 – 715714-6, 2008.

4) J. Wang and Q. Wang, Erbium-doped fiber amplifiers: A short review on technology and performance, Optik, vol. 124, no. 24, pp. 6611-6616, 2013.

5) H. Masuda and A. Takada, High-gain two-stage amplification with erbium-doped fiber amplifier, Electronics Letters, vol. 26, no. 10, pp. 661-662, 1990.

6) J.M.P. Delavaux and J.A. Nagel, Multi-stage erbium-doped fiber amplifier designs, Journal of Lightwave Technology, vol. 13, no. 5, pp. 703-720, 1995.

7) P. Myslinski, D. Nguyen and J. Chrostowski, Effects of concentration on the performance of erbium-doped fiber amplifiers, Journal of Lightwave Technology, vol. 15, no. 1, pp. 112-120, 1997.

8) D.D. Pradhan and A. Mandloi, Design Optimization of EDFA for 16 × 10 Gbps Data Rate DWDM System Using Different Pumping Configurations, Wireless Personal Communications, vol. 106, no. 4, pp. 2079-2086, 2019.

9) I. Lavrinovica, A. Supe, and J. Porins, Experimental Measurement of Erbium-Doped Optical Fibre Charecteristics for Edfa Performance Optimization, Latvian Journal of Physics and Technical Sciences, vol. 56, no. 2, pp. 33–41, 2019.

10) K. Zakis, S. Spolītis, T. Salgals, L. Ģēģere, M. Parfjonovs, D. Prigunovs, V. Bobrovs, and A. Supe, Experimental Characterization of Signal Gain Evolution in Cladding-pumped Doped Fiber Amplifier, 2023 Photonics & Electromagnetics Research Symposium (PIERS), Prague, Czech Republic, pp. 754-758, 2023.

11) S. Jalilpiran, J. Lefebvre, Y. Messaddeq, and S. LaRochelle, Analysis of Signal Excited-State Absorption for Improving Extended L-band Erbium-Doped Fibers, Optics Letters, vol. 49, no. 20, pp. 5715-5718, 2024.

12) D. Gandhi, Evaluation of Gain and Noise Figure Spectrum of EDFA by Optimizing its Parameters with Different Pumping Schemes in the Scenario of WDM System, International Conference on Emerging Technology Trends in Electronics Communication and Networking, pp. 136-146, 2020.

13) S. Semmalar and S.Malarkkan, Output signal power analysis in erbium-doped fiber amplifier with pump power and length variation using various pumping techniques, ISRN Electronics, vol. 2013, pp. 312707-1 – 312707-6, 2013.

14) M.K. Awsaj, H.H. Goktas, M. Yucel and M.K. Awsaj, Gain and noise figure analysis of erbium doped fiber amplifier based on double pass configuration using forward pumping, IOP Conference Series: Materials Science and Engineering, vol. 1094, pp. 012095-1 – 012095-9, 2021.

15) Y. Liu, X. Liu, L. Liu, Y. Zhang, M. Cai, L. Yi, W. Hu and Q. Zhuge, Modeling EDFA gain: approaches and challenges, Photonics, vol. 8, no. 417, pp. 1-9, 2021.

16) R. Róka, Simulation of the optical erbium doped fiber amplification for performance analysis, Journal of Electrical Engineering, vol. 72, no. 3, pp. 168-175, 2021.

17) R. Giles and E. Desurvire, Modeling erbium-doped fiber amplifiers, Journal of Lightwave Technology, vol. 9, pp. 271-283, 1991.

18) P.C. Becker, N.A. Olsson and J.R. Simpson, Erbium-doped fiber amplifiers fundamentals and technology, Academic Press, 1999.

19) Z. Zhai et al., Temperature-Dependent Study on L-Band EDFA Characteristics Pumped at 980 nm and 1480 nm in Phosphorus and Aluminum-Rich Erbium-Doped Silica Fibers, Journal of Lightwave Technology, vol. 40, no. 14, pp. 4819–4828, 2022.

20) J.-B. Trinel et al., Few-mode erbium-doped fiber amplifier based on a multi-inclusions core optical fiber, Optics Express, vol. 31, no. 3, pp. 4444–4453, 2023.

21) H. Lao et al., Dual-Stage Double-Pass Extended L-Band Erbium-Doped Fiber Amplifier with Improved Gain Performance, Photonics, vol. 10, no. 11, 1266, 2023.

22) Z. Gu et al., M-type refractive index profile erbium-doped fiber for high-efficiency multicore EDFA, Optics Express, vol. 32, no. 5, pp. 7564–7573, 2024.

23) H. Li et al., Tunable gain clamping L-band erbium-doped fiber amplifier based on FBG and BBM, Optical Fiber Technology, vol. 88, 103823, 2024.

24) Y. Zhang et al., High-power, low-noise, high-gain few-mode fiber amplifier, Optics & Laser Technology, vol. 169, 110008, 2024.